NANO LETTERS

pubs.acs.org/NanoLett

Mini Review

# A New Approach to Designing High-Sensitivity Low-Dimensional Photodetectors

Mohsen Rezaei, Simone Bianconi, Lincoln J. Lauhon, and Hooman Mohseni*

Cite This: https://doi.org/10.1021/acs.nanolett.1c03665

Read Online

ACCESS | Metrics & More | Article Recommendations

**ABSTRACT:** Photodetectors fabricated from low-dimensional materials such as quantum dots, nanowires, and two-dimensional materials show tremendous promise based on reports of very high responsivities. However, it is not generally appreciated that maximizing the internal gain may compromise the detector performance at low light levels, reducing its sensitivity. Here, we show that for most low-dimensional photodetectors with internal gain the sensitivity is determined by the junction capacitance. Thanks to their extremely small junction capacitances and reduced charge screening, low-dimensional materials and devices provide clear advantages over bulk semiconductors in the pursuit of high-sensitivity photodetectors. This mini-review describes and validates a method to estimate the capacitance from external photoresponse measurements, providing a straightforward approach to extract the device sensitivity and benchmark against physical limits. This improved physical understanding can guide the design of low-dimensional photodetectors to effectively leverage their unique advantage and achieve sensitivities that can exceed that of the best existing photodetectors.

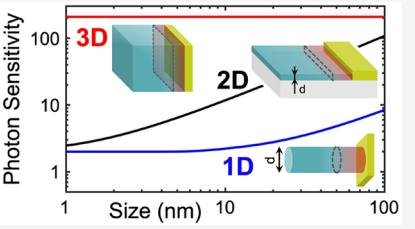


**KEYWORDS:** *Photodetectors, Low-dimensional materials, Sensitivity, Capacitance, Responsivity, Quantum efficiency*

Downloaded via NORTHWESTERN UNIV on November 30, 2021 at 02:58:44 (UTC).
See https://pubs.acs.org/sharingguidelines for options on how to legitimately share published articles.

## INTRODUCTION

Low-dimensional materials including quantum dots, nanowires, and two-dimensional (2D) materials have been extensively used to fabricate photodetectors operating at wavelengths ranging from UV to infrared.[1−4] The peculiar electro-optical physics of these materials and the related devices provide mechanisms to realize large internal gain, thereby enabling large photoresponsivity. The responsivity $\mathcal{R}$ of a photoconductive detector is defined as the ratio of the output photocurrent to the input optical power, and is proportional to the internal gain $\beta$:

$$\mathcal{R} = \frac{\lambda q}{hc}\eta\beta \tag{1}$$

where $q$ is the electron charge, $hc/\lambda$ is the energy of the incoming photons, and $\eta$ is the internal quantum efficiency. Thus, maximizing the internal gain maximizes the responsivity, which is often considered an end goal.

It is true that signal amplification within the photodetector material, i.e. internal gain, is necessary in applications where the goal is detecting small optical powers, since the signal level needs to be raised well above the noise of the read-out electronics in order to achieve detection with high signal-to-noise ratio (SNR). For most such applications, however, sensitivity and detectivity are the key performance metrics because they describe the detection efficiency at a system level. The sensitivity describes the smallest signal that can be detected, and a useful measure of the sensitivity is the noise-equivalent power (NEP), which represents the smallest incident power that can be detected with an SNR = 1:[5,6]

$$\mathrm{NEP} = \frac{I_n}{\mathcal{R}} \tag{2}$$

where $I_n$ is the rms noise current. By convention, the NEP is often reported in units of $\mathrm{W}/\sqrt{\mathrm{Hz}}$ for a fixed reference bandwidth of 1 Hz.[5] The specific detectivity is simply the inverse of the NEP, normalized to the square root of the area $A$ and bandwidth (BW) of the detector:

$$D^* = \frac{\sqrt{A\mathrm{BW}}}{\mathrm{NEP}} \tag{3}$$

It is important to point out that specific detectivity as a detector figure of merit was constructed to enable comparison of the ultimate performance limits of different bulk materials, and is not a reliable relative indicator of detection performance when the region of illumination is larger than the size of the responsive region. As such, we do not recommend the use of specific detectivity as a performance figure of merit for detectors based on low-dimensional and nanoscale materials, where the

Received: September 21, 2021
Revised: November 10, 2021

ACS Publications © XXXX American Chemical Society

characteristic dimensions of the detectors are typically smaller than the wavelength of light, since normalizing to a subwavelength detector area can produce misleading and exaggerated specific detectivity values. An effective measure of the sensitivity of a detector is the noise-equivalent number of photons, NEPh, defined as the smallest number of photons that can be detected in one acquisition with an SNR = 1: detectors with NEPh $\leq$ 1 are designated single-photon detectors (SPD).[7,8] Unlike the NEP, the NEPh takes the dynamics of the detector into account and is normalized to the energy of the detected photons:

$$\mathrm{NEPh} = \frac{\mathrm{NEP}}{hc/\lambda} T_{\mathrm{int}} = \frac{I_n}{q\eta\beta} T_{\mathrm{int}} \tag{4}$$

where $T_{\mathrm{int}}$ the integration time of the readout circuitry.

A review of the research literature on low-dimensional photodetectors suggests that a large responsivity is commonly conflated with a high sensitivity, when in fact a focus on maximizing responsivity may actually *reduce* the sensitivity.[9,10] It is evident from eq 4 that a high gain (or responsivity) only improves sensitivity as long as it does not simultaneously affect the noise and bandwidth of the device. Indeed, while several low-dimensional detectors with record-high responsivities have been reported, none of these devices has yet surpassed the performance of bulk photodetectors on the key metric of sensitivity.[5−7] In this mini-Review, we identify common gain mechanisms in low-dimensional photodetectors, derive the design principles that maximize the sensitivity, and validate the approach by benchmarking prior reports in the literature. We confirm the promise of low-dimensional materials for high sensitivity photodetectors and provide a path to realize the limits of performance.

## GAIN MECHANISMS IN LOW-DIMENSIONAL PHOTODETECTORS

While low-dimensional detectors employ a variety of amplification mechanisms,[11] the vast majority can be understood as transistors, particularly floating-base junction[4,12] or floating-gate field effect[13,14] phototransistors. In such detectors, light modulates a space charge region (SCR) that acts as a barrier to the transport of majority carriers. The SCR is induced by charge transfer at a heterointerface, such as a type-II semiconductor junction[15,16] or Schottky junction,[17] or at any surface with occupied defect states.[18] Upon absorption of a photon, an electron−hole pair is generated and the minority carrier migrates to SCR, modifying the concentration of fixed charge in the trap states. The reduction in the barrier to majority carrier transport produces a large increase in current.[4,12] This amplification mechanism has been reported for a large number of photodetectors with gain based on low-dimensional materials.[4,12−14,17,18]

As an example, Figure 1 shows a schematic representation of typical gain mechanisms in nanowire detectors. In Figure 1a, surface trap states create a depleted SCR that extends into the bulk of the nanowire, narrowing the conductive channel across the nanowire axis. Photogenerated minority carriers (holes in this case) migrate to the surface, occupying the trap states and decreasing the depletion width of the SCR, thereby increasing the size of the conductive channel and triggering a large photocurrent. A similar mechanism is observed in core−shell nanowire structures, where the SCR is created by the radial heterojunction.[19,20] These devices can be modeled as floating-gate field effect transistors in which the modulation of the width of the SCR changes the conductance of the detector.[4,12] In Figure 1b, the interface between an n-type nanowire and the electrode forms a Schottky barrier, which limits the flow of electrons. Here too, the photogenerated minority carriers (holes) accumulate in the SCR generated by the metal−semiconductor junction and lower the potential barrier, greatly increasing the flow of majority carriers (electrons), similarly to the gain mechanism of heterojunction phototransistors.[17] It is worth noting that both mechanisms may coexist in nanowires detectors, with the dominant of the two contributions depending on the device design.[20,21]

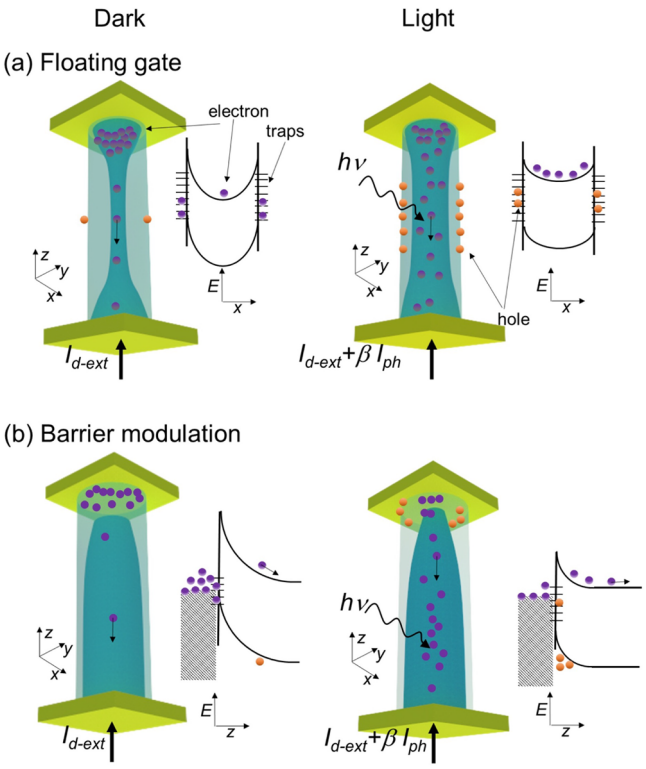


**Figure 1.** Schematic diagram of the gain mechanisms in nanowire detectors. (a) Nanowire detector with surface depletion. (b) Nanowire detector with a Schottky potential barrier.

While Figure 1 depicts the gain mechanisms in nanowire (1D) photodetectors, similar gain mechanisms are also observed in detectors fabricated from 0D and 2D materials. In 2D materials, the potential barrier modulated by photogenerated carriers is typically created at the contact electrodes[22] or at heterojunction interfaces between different 2D materials.[15] Quantum dots (0D) photodetectors serve to localize (trap) photogenerated charges, which then modulate the transport of free charge carriers. To fabricate photodetectors, quantum dots are often formed into photoconductive films, serving as photoconductors, photodiodes, or the channel of phototransistors; here, the photoconductive gain is created by the modulation of the flow of the majority carrier by the trapped photogenerated minority carriers.[23] Alternatively, quantum dots are employed to photosensitize a semiconducting supporting layer, forming a photovoltage field effect transistor.[10,13,14] As such, most 0D detectors are actually "mixed-dimensional", since they either form photoconductive films or couple to 2D films or bulk semiconductor devices.


https://doi.org/10.1021/acs.nanolett.1c03665
Nano Lett. XXXX, XXX, XXX−XXX

It is also important to note that unlike in conventional semiconductor devices, the geometry of the SCR in detectors based on low-dimensional materials can vary significantly depending on the influence of defects and trap states. As showcased in Figure 1, an SCR can be induced at the surface by the occupation of surface states, as well as at a heterojunction interface by both band offsets and interface states. Because the surface-to-volume ratio of nanoscale materials is drastically higher than that of conventional photodetectors, charged surface states often control the dynamics of the SCR, therefore governing the above-mentioned gain mechanisms.[12] As a result, a comprehensive characterization of the density and occupation of the trap states at the surfaces and interfaces as well as the band alignment at the junctions is required in order to analytically calculate the SCR capacitance of detectors based on low-dimensional materials.[6,24,25] This characterization is often complicated, costly, and prone to errors. Alternatively, for a substantial fraction of reported photodetectors with gain based on low-dimensional materials, the SCR capacitance can be estimated from other device characteristics, as we will discuss in detail in the following sections.

## SENSITIVITY OF LOW DIMENSIONAL PHOTODETECTORS

For these low-dimensional detectors employing a gain mechanism analogous to that of phototransistors, the capacitance of the SCR ($C_{SCR}$) relates the magnitude of the change in barrier potential induced by the accumulation of a given number of photogenerated spatially localized charges, and is therefore the key parameter governing the device amplification and sensitivity. $C_{SCR}$ is related to the response time of the detector, $\tau$, which is well approximated by the RC time constant of a floating-base or floating-gate phototransistor.[12,17,26]

$$\tau \approx r_d C_{SCR} \tag{5}$$

where $r_d$ is the dynamic resistance of the photodetector, defined as $r_d = dV/dI$.[27] For the case of a heterojunction photodetector in low-light conditions, such as when sensing a small number of photons, $r_d$ can be expressed as $r_d = V_t/i_D$, with $V_t = kT/q$ the thermal voltage, and $i_D$ is the internal dark current before amplification, related to the measured external dark current $I_D$ as $i_D = I_D/\beta$.[27] Similarly, for the case of floating-gate field effect phototransistors, where the gate cannot be reset externally, the dynamic resistance is governed by the gate leakage current $i_L$, i.e. $r_d = V_t/i_L$.

Notably, the response time of a photodetector is governed by a series of device properties, such as capacitance, dynamic resistance, recombination rate, and gain, where the dominant contribution determining the speed of the device depends on the device architecture and material properties.[26] While the response time of most photodetectors with high-sensitivity is RC-limited, other factors can limit the device speed. As an example, there are several reports of slow detectors with high gain, enabled by long-lived traps in 2D materials.[1] However, we note that the definition of sensitivity as the NEPh incorporates the device response time, which naturally implies that extremely slow single-photon detectors could only operate at unrealistically small photon fluxes. In addition, at a given sensitivity, a slower detector must have a lower dark current than a faster detector. To connect with practical applications, the formulation presented here assumes a detector response time determined by the RC time constant, which we believe to be the optimal design point for realistic applications requiring high sensitivity.

The bandwidth of a detector determines its noise contribution to sensitivity, as shown in eqs 2 and 4. Assuming shot noise-limited detector operation, the noise can therefore be expressed as a function of dark current, gain, and $C_{SCR}$.[28] This enables one to solve eq 4 for the NEPh and to express the detector sensitivity in a simple form that illuminates key design principles:[28]

$$\mathrm{NEPh} = \frac{1}{\eta}\left(1 + \sqrt{1 + 4\alpha\frac{C_{SCR}}{C_0}}\right) \tag{6}$$

where $C_0 = q/V_t$ is the fundamental thermal capacitance, and the parameter $\alpha$ is unity for the case of floating-base bipolar phototransistors and $\alpha = i_D/i_L$ for floating-gate field effect phototransistors. Notably, for most photon counting applications, such as photon arrival statistics and quantum communication, the Poisson noise related to the photons random arrival time is decoupled from the detector noise and, therefore, typically neglected in the sensitivity estimation.[7] This in turn leads to a modified expression for eq 6: $\mathrm{NEPh} = 1/\eta\sqrt{4\alpha C_{SCR}/C_0}$. While the application will dictate which expression for the detector sensitivity is most appropriate, we note that the two expressions closely match for NEPh $\gg 1$ but deviate significantly near NEPh $\approx 1$.

Equation 6 shows that the sensitivity can be maximized by decreasing the SCR capacitance and increasing the quantum efficiency. Low-dimensional materials offer an unparalleled avenue toward detectors with extremely low capacitance and therefore high sensitivity. This is in part owing to the characteristic nanoscale dimensions enabling very small junction cross sections, such as in nanowires[21] and lateral-junction thin film detectors.[3,29] In addition, the electrostatics of charge screening in low-dimensional structures considerably extends the SCR region beyond the corresponding depletion width in bulk materials,[30,31] hence contributing to reducing the junction capacitance. Figure 2 showcases the advantage of low-dimensional materials for photodetection: decreasing the diameter of nanowires (1D) or the thickness of 2D materials enables significant improvements in sensitivity. Here, $C_{SCR}$ is estimated

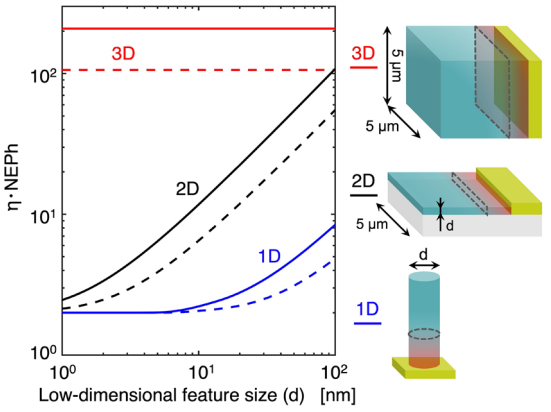


**Figure 2.** Sensitivity of low-dimensional photodetectors (1D and 2D) compared to bulk (3D). Sensitivity is expressed in NEPh multiplied by internal quantum efficiency, as a function of the low-dimensional feature size $d$ (i.e., thickness for 2D materials, diameter for nanowires). The solid lines represent the sensitivity at 300 K, while the dashed lines represent the sensitivity at 77 K. The lateral dimension is 5 $\mu$m, the doping 1$e$19 cm$^{-3}$, and the voltage bias 2 V.


https://doi.org/10.1021/acs.nanolett.1c03665
Nano Lett. XXXX, XXX, XXX−XXX

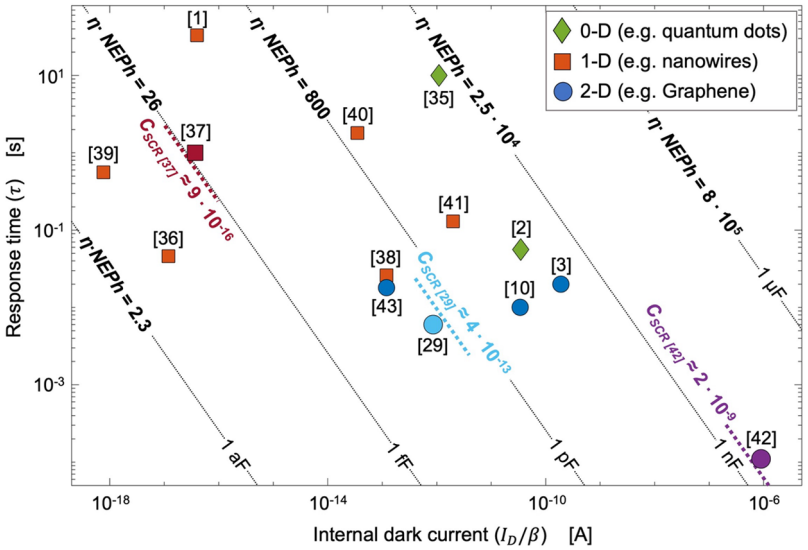


**Figure 3.** Response time and internal dark current of detectors based on 0D (diamonds), 1D (squares), and 2D (circles) materials. Dashed lines represent constant SCR capacitance, and hence constant sensitivity lines. The three dashed colored lines represent the validated values of the capacitances of the devices of the corresponding color.

**Table 1. Device Parameters Used in the Calculations for Figure 3, Including Estimated Capacitance and Sensitivity**[a]

| ref | $\tau$ [s] | $I_D$ [A] | Gain ($\beta$) | $C_{SCR-model}$ | Area [$\mu m^2$] | $C_{SCR-geom.}$ | $\eta$· NEPh |
|---|---|---|---|---|---|---|---|
| 1 | 33 | $8.0 \times 10^{-9}$ | $2.0 \times 10^{8}$ | ~51 fF | – | – | ~180 |
| 2 | $5.6 \times 10^{-2}$ | $1.2 \times 10^{-7}$ | $3.4 \times 10^{3}$ | ~75 pF | – | – | ~7000 |
| 3 | $2.0 \times 10^{-2}$ | $2.6 \times 10^{-9}$ | $1.4 \times 10^{1}$ | ~150 pF | – | – | ~9800 |
| 10 | $1.0 \times 10^{-2}$ | $3.5 \times 10^{-3}$ | $1.0 \times 10^{8}$ | ~13 pF | – | – | ~2900 |
| 29 | $6.0 \times 10^{-3}$ | $2.0 \times 10^{-8}$ | $2.3 \times 10^{4}$ | ~200 fF | 6 × 10 | ~370 fF | ~ 360 |
| 35 | $1.0 \times 10^{1}$ | $2.0 \times 10^{-10}$ | $1.9 \times 10^{2}$ | ~410 pF | – | – | $\sim 1.6 \times 10^{4}$ |
| 36 | $4.6 \times 10^{-2}$ | $1.0 \times 10^{-13}$ | $8.5 \times 10^{3}$ | ~21 aF | – | – | ~4.8 |
| 37 | 1 | $1.0 \times 10^{-13}$ | $2.7 \times 10^{3}$ | ~1.4 fF | 0.5 × 2 | ~0.89 fF | ~ 31 |
| 38 | $2.6 \times 10^{-2}$ | $1.0 \times 10^{-8}$ | $8.4 \times 10^{4}$ | ~120 fF | 0.8 × 100 | ~92 fF | ~280 |
| 39 | $5.6 \times 10^{-1}$ | $2.0 \times 10^{-11}$ | $2.6 \times 10^{7}$ | ~17 aF | – | – | ~4.4 |
| 40 | 1.8 | $5.0 \times 10^{-8}$ | $1.4 \times 10^{6}$ | ~2.5 pF | – | – | ~1300 |
| 41 | $1.3 \times 10^{-1}$ | $4.7 \times 10^{-8}$ | $2.3 \times 10^{4}$ | ~9.9 pF | – | – | ~2500 |
| 42 | $1.1 \times 10^{-4}$ | $1.2 \times 10^{-5}$ | 13 | ~3.8 nF | 500 × 158 | ~2.4 nF | $\sim 5 \times 10^{4}$ |
| 43 | $1.8 \times 10^{-2}$ | $2.0 \times 10^{-10}$ | $1.6 \times 10^{3}$ | ~85 fF | – | – | ~240 |

[a]For a few devices,[29,37,38,42] the SCR capacitances estimated from the geometric junction data are compared to those extracted using the model.

by using a parallel plate capacitor approximation and employing the model proposed by Ilatikhameneh et al.[31] to calculate the depletion thickness of the SCR for all three different dimensionalities. The sensitivity is then determined from $C_{SCR}$ using eq 6. For the typical conditions simulated in Figure 2 ($10^{19}$ $cm^{-3}$ doping concentration and 2 V bias), as an example, low-dimensional materials can enhance the sensitivity of up to 2 orders of magnitude over bulk, thanks to the combined effect of the reduced junction cross section and enhanced charge depletion in the SCR.

Obviously, reducing $C_{SCR}$ in low-dimensional materials may come at the cost of a decrease in quantum efficiency due to the smaller absorbing volume, highlighting a key design trade-off in this class of photodetectors, as we will discuss below.

As discussed above, the SCR in low-dimensional materials is profoundly affected by the presence of traps, as showcased in Figure 1, and the concentration of defects at the surface and interfaces, as well as the band alignment at the junctions play a crucial role in determining the value of the SCR capacitance.[6,24,25] As such, it is extremely beneficial to be able to estimate the value of this capacitance from measurable device parameters, without the need to investigate the internal structure and composition of the detectors. By rearranging the expressions for the RC time constant and dynamic resistance, the SCR capacitance can be expressed in terms of easily measured parameters:

$$C_{SCR} = \frac{\tau I_D}{\beta \alpha V_t} \tag{7}$$

The sensitivity of a detector can therefore be estimated from its response time, dark current, gain, and operating temperature. Some of these metrics are often included in reports of detector performance, yet comparisons can still be misleading in the absence of a quantitative evaluation of their combined impact on the device sensitivity. The assumption that high gain leads to high sensitivity is one such example. Furthermore, because it is challenging to directly measure the sensitivity or the SCR capacitance, they are not frequently reported—or correctly characterized—in the literature.[6] In contrast, eq 7 allows one to estimate the sensitivity from easily measured device parameters like dark current, gain, and response time. As an example, a


https://doi.org/10.1021/acs.nanolett.1c03665
Nano Lett. XXXX, XXX, XXX−XXX

simple and effective method to derive the internal gain of a photodetector is from its noise spectrum.[32−34] Notably, measuring the noise floor of a detector is an especially accessible measurement when such noise is amplified by gain, such as in these cases.

The immediate utility of this approach is demonstrated in the comparison of the sensitivity of photodetectors based on different low-dimensional materials in Figure 3; plotting sensitivity in terms of NEPh multiplied by internal quantum efficiency also enables direct comparison with state-of-the-art technologies. Here, eqs 6 and 7 are used to compare the performance of more than a dozen devices representing three types of low-dimensional detectors: diamonds indicate 0D detectors,[2,35] squares indicate 1D detectors,[1,36−41] and circles indicate 2D detectors.[3,10,29,42,43] The dashed lines represent the relationship between response time and internal dark current for constant SCR capacitances defined in eq 7. According to eq 6, each of these lines also corresponds to a specific value of NEPh at room temperature, for a given quantum efficiency. The specific device parameters used in these calculations are presented in Table 1.

Figure 3 showcases the ease of quantitatively comparing the performance of detectors based on different low-dimensional materials and designs, using only the device external parameters according to eqs 6 and 7. For example, the detectors reported in refs 29 and 1 have similar levels of sensitivity, despite the first having a gain around 300 times lower than the second, while being almost 4 orders of magnitude faster, at the same dark current. This comparison also exemplifies a situation where higher gain does not lead to higher sensitivity, as discussed in the previous sections.

To showcase the efficacy of the proposed approach, we also show in Table 1 that the capacitance values estimated from the geometric junction characteristics using a parallel plate capacitor approximation ($C_{SCR-geom.}$) are in relatively good agreement with the capacitance values estimated using eq 7 ($C_{SCR-model}$). For three of the devices[29,37,42] in Figure 3, enough information on the geometrical and material properties of the junctions was provided (or could be inferred from scanning electron microscopy and other characterization techniques) to enable direct estimation of the SCR capacitance. The details of the two methods for estimating the SCR capacitance are shown in Table 1, where the geometric estimation of the capacitance, $C_{SCR-geom}$, is compared with $C_{SCR-model}$, calculated from the response time, dark current, and gain, according to eq 7. Despite the rough parallel plate capacitor approximation employed, the two set of values are in reasonably good agreement for values of $C_{SCR}$ spanning over 6 orders of magnitude, demonstrating the validity of our proposed approach. Notably, no geometric estimation of the SCR capacitance has been performed for 0D detectors: as mentioned above, most reported 0D detectors are actually "mixed-dimensional", either forming photoconductive films or coupling to 2D films or bulk semiconductor devices.[10,13,23] This case demonstrates the challenges of developing a single approximation of the geometric capacitance that is appropriate for all types of low-dimensional photodetectors, showcasing the advantage of the approach presented here for estimating the capacitance of the SCR from measured device parameters.

In addition, it is interesting to note that since speed and the internal dark current are proportional in photoconductors, then external factors that affect either of these, such as changes in temperature, environment, or optical biasing, will cause the device data point in Figure 3 to translate along a line of constant sensitivity (i.e., parallel to the dashed lines) according to eq 7. An example of this effect is offered by the behavior of the response time of a ZnO nanowire detector reported in ref 44 when operated in vacuum compared to in ambient air. Here, the ratio of the detector gain in air to that in vacuum is $\beta_{vac}/\beta_{air} \approx 700$, and the ratio of the external dark currents is only $I_{D_{air}}/I_{D_{vac}} \approx 3.4$.[44] As a result, the ratio between the internal dark currents $i_{D_{air}}/i_{D_{vac}} = I_{D_{air}}/I_{D_{vac}} \cdot \beta_{vac}/\beta_{air} \approx 2400$. By rearranging the terms in eq 7, our model enables estimation of the ratio between the response times in the two conditions, as $i_{D_{air}}/i_{D_{vac}} = \tau_{vac}/\tau_{air} \approx 2400$. Indeed, from the direct photoresponse measurements, the ratio of the response times in the two conditions is around $5 \times 10^3$,[44] which is in fairly good agreement with that estimated by the model.

In summary, the simple model proposed in eq 6 shows that the sensitivity of low-dimensional detectors can be increased by making the SCR capacitance as small as possible and by increasing quantum efficiency. Furthermore, the model provides researchers with a powerful tool for the design of novel high-sensitivity photodetectors based on low-dimensional materials. The recommended iterative design approach is as follows:

1. Measure the dark current, response time, and gain of a set of detector prototype devices.
2. Use these measured device parameters to estimate the value of the SCR capacitance of the devices from eq 7.
3. Extract the internal quantum efficiency from an appropriate characterization of the photoresponsivity of the devices (as discussed below).
4. Estimate the sensitivity of the detectors from the SCR capacitance and internal quantum efficiency, using eq 6.
5. Apply the insight gained on the sensitivity of the devices to guide the design of an improved set of prototypes, and reiterate the process.

Significantly, eq 6 also highlights a key design trade-off: smaller detectors tend to have lower quantum efficiencies due to the smaller overlap of the incident optical modes with the small detector volume. In general, all detectors with characteristic sizes smaller than the wavelength of photons are confronted by severe limitations in light absorption.[8,45] In order to optimize the detector design for maximizing sensitivity, it is therefore crucial to combine the estimation of the SCR capacitance described by eq 7 with an accurate characterization of the detector quantum efficiency. In particular, internal quantum efficiency can be extracted from appropriate calibrated photoresponsivity measurements[10,13,45] that avoid errors such as normalizing the illumination power to a subwavelength detector area, as these might result in artificial enhancement of the detector performance. Finally, a number of proposed light coupling enhancement strategies can help overcome this intrinsic trade-off, provided that they can maintain a high quantum efficiency in concentrating the light into subwavelength detectors.[46−48]

## CONCLUSION

This work offers a unified approach to guide the design and development of high-sensitivity photodetectors based on low-dimensional materials. For low-dimensional detectors employing gain mechanisms analogous to that of phototransistors, the total capacitance of SCR is the key factor in determining the sensitivity. This capacitance can be estimated from external photoresponse measurements, providing a straightforward approach to extract the device sensitivity. The present study


https://doi.org/10.1021/acs.nanolett.1c03665
Nano Lett. XXXX, XXX, XXX−XXX

focuses on highly sensitive detectors for low-light applications, where the goal is to reliably detect a small number of photons. Detectors based on low-dimensional materials exhibit enormous potential owing to their intrinsically small junction capacitances, but it is essential to concomitantly implement strategies to improve light coupling and quantum efficiency. Finally, we note that low-dimensional detectors are attractive for other performance characteristics beyond sensitivity, including the potential for low-cost fabrication as well as their ease of integration on hybrid and unconventional platforms.

## AUTHOR INFORMATION


### Corresponding Author

**Hooman Mohseni** − *Department of Electrical and Computer Engineering, Northwestern University, Evanston, Illinois 60208, United States*; Email: hmohseni@northwestern.edu

### Authors

**Mohsen Rezaei** − *Department of Electrical and Computer Engineering, Northwestern University, Evanston, Illinois 60208, United States*

**Simone Bianconi** − *Department of Electrical and Computer Engineering, Northwestern University, Evanston, Illinois 60208, United States*; orcid.org/0000-0002-3828-6513

**Lincoln J. Lauhon** − *Department of Material Science and Engineering, Northwestern University, Evanston, Illinois 60208, United States*; orcid.org/0000-0001-6046-3304

Complete contact information is available at: https://pubs.acs.org/10.1021/acs.nanolett.1c03665


### Notes

The authors declare no competing financial interest.

## ACKNOWLEDGMENTS

S.B. gratefully acknowledges support from the Ryan Fellowship and the International Institute for Nanotechnology at Northwestern University. L.L. acknowledges support of NSF DMR 1905768 and NSF DMR 1720139. This work was partially supported by ARO Award W911NF1810429 and NIH Award R21EY029516.

## REFERENCES


(1) Soci, C.; Zhang, A.; Xiang, B.; Dayeh, S. A.; Aplin, D.; Park, J.; Bao, X.; Lo, Y.-H.; Wang, D. ZnO nanowire UV photodetectors with high internal gain. *Nano Lett.* **2007**, *7*, 1003−1009.

(2) Konstantatos, G.; Howard, I.; Fischer, A.; Hoogland, S.; Clifford, J.; Klem, E.; Levina, L.; Sargent, E. H. Ultrasensitive solution-cast quantum dot photodetectors. *Nature* **2006**, *442*, 180−183.

(3) Hu, P.; Wen, Z.; Wang, L.; Tan, P.; Xiao, K. Synthesis of few-layer GaSe nanosheets for high performance photodetectors. *ACS Nano* **2012**, *6*, 5988−5994.

(4) Zhang, H.; Babichev, A.; Jacopin, G.; Lavenus, P.; Julien, F.; Yu; Egorov, A.; Zhang, J.; Pauporté, T.; Tchernycheva, M. Characterization and modeling of a ZnO nanowire ultraviolet photodetector with graphene transparent contact. *J. Appl. Phys.* **2013**, *114*, 234505.

(5) Rogalski, A. *Infrared detectors*; CRC Press: Boca Raton, FL, 2010.

(6) Fang, Y.; Armin, A.; Meredith, P.; Huang, J. Accurate characterization of next-generation thin-film photodetectors. *Nat. Photonics* **2019**, *13*, 1−4.

(7) Ma, J.; Masoodian, S.; Starkey, D. A.; Fossum, E. R. Photon-number-resolving megapixel image sensor at room temperature without avalanche gain. *Optica* **2017**, *4*, 1474−1481.

(8) Bianconi, S.; Mohseni, H. Recent advances in infrared imagers: toward thermodynamic and quantum limits of photon sensitivity. *Rep. Prog. Phys.* **2020**, *83*, 044101.

(9) Soci, C.; Zhang, A.; Bao, X.-Y.; Kim, H.; Lo, Y.; Wang, D. Nanowire photodetectors. *J. Nanosci. Nanotechnol.* **2010**, *10*, 1430−1449.

(10) Konstantatos, G.; Badioli, M.; Gaudreau, L.; Osmond, J.; Bernechea, M.; De Arquer, F. P. G.; Gatti, F.; Koppens, F. H. Hybrid graphene−quantum dot phototransistors with ultrahigh gain. *Nat. Nanotechnol.* **2012**, *7*, 363−368.

(11) Koppens, F.; Mueller, T.; Avouris, P.; Ferrari, A.; Vitiello, M.; Polini, M. Photodetectors based on graphene, other two-dimensional materials and hybrid systems. *Nat. Nanotechnol.* **2014**, *9*, 780.

(12) Garrido, J.; Monroy, E.; Izpura, I.; Munoz, E. Photoconductive gain modelling of GaN photodetectors. *Semicond. Sci. Technol.* **1998**, *13*, 563.

(13) Adinolfi, V.; Sargent, E. H. Photovoltage field-effect transistors. *Nature* **2017**, *542*, 324−327.

(14) Goossens, S.; Navickaite, G.; Monasterio, C.; Gupta, S.; Piqueras, J. J.; Perez, R.; Burwell, G.; Nikitskiy, I.; Lasanta, T.; Galán, T. Broadband image sensor array based on graphene−CMOS integration. *Nat. Photonics* **2017**, *11*, 366.

(15) Flöry, N.; Ma, P.; Salamin, Y.; Emboras, A.; Taniguchi, T.; Watanabe, K.; Leuthold, J.; Novotny, L. Waveguide-integrated van der Waals heterostructure photodetector at telecom wavelengths with high speed and high responsivity. *Nat. Nanotechnol.* **2020**, *15*, 118−124.

(16) Sangwan, V. K.; Kang, J.; Lam, D.; Gish, J. T.; Wells, S. A.; Luxa, J.; Male, J. P.; Snyder, G. J.; Sofer, Z.; Hersam, M. C. Intrinsic carrier multiplication in layered Bi 2 O 2 Se avalanche photodiodes with gain bandwidth product exceeding 1 GHz. *Nano Res.* **2021**, *14*, 1961−1966.

(17) Hu, Y.; Zhou, J.; Yeh, P.-H.; Li, Z.; Wei, T.-Y.; Wang, Z. L. Supersensitive, fast-response nanowire sensors by using Schottky contacts. *Adv. Mater.* **2010**, *22*, 3327−3332.

(18) Kim, C.-J.; Lee, H.-S.; Cho, Y.-J.; Kang, K.; Jo, M.-H. Diameter-dependent internal gain in ohmic Ge nanowire photodetectors. *Nano Lett.* **2010**, *10*, 2043−2048.

(19) Yang, Z.; Guo, L.; Zu, B.; Guo, Y.; Xu, T.; Dou, X. CdS/ZnO core/shell nanowire-built films for enhanced photodetecting and optoelectronic gas-sensing applications. *Adv. Opt. Mater.* **2014**, *2*, 738−745.

(20) Sett, S.; Ghatak, A.; Sharma, D.; Kumar, G. P.; Raychaudhuri, A. Broad band single germanium nanowire photodetectors with surface oxide-controlled high optical gain. *J. Phys. Chem. C* **2018**, *122*, 8564−8572.

(21) Ren, D.; Meng, X.; Rong, Z.; Cao, M.; Farrell, A. C.; Somasundaram, S.; Azizur-Rahman, K. M.; Williams, B. S.; Huffaker, D. L. Uncooled photodetector at short-wavelength infrared using InAs nanowire photoabsorbers on InP with p−n heterojunctions. *Nano Lett.* **2018**, *18*, 7901−7908.

(22) Murthy, A. A.; Stanev, T. K.; Cain, J. D.; Hao, S.; LaMountain, T.; Kim, S.; Speiser, N.; Watanabe, K.; Taniguchi, T.; Wolverton, C.; Stern, N. P.; Dravid, V. P.; et al. Intrinsic transport in 2D heterostructures mediated through h-BN tunneling contacts. *Nano Lett.* **2018**, *18*, 2990−2998.

(23) Liu, M.; Yazdani, N.; Yarema, M.; Jansen, M.; Wood, V.; Sargent, E. H. Colloidal quantum dot electronics. *Nature Electronics* **2021**, *4*, 548−558.

(24) Cai, Y.; Zhang, G.; Zhang, Y.-W. Layer-dependent band alignment and work function of few-layer phosphorene. *Sci. Rep.* **2015**, *4*, 1−6.

(25) Pierucci, D.; et al. Band alignment and minigaps in monolayer MoS2-graphene van der Waals heterostructures. *Nano Lett.* **2016**, *16*, 4054−4061.

(26) Helme, J. P.; Houston, P. A. Analytical modeling of speed response of heterojunction bipolar phototransistors. *J. Lightwave Technol.* **2007**, *25*, 1247−1255.

(27) Sze, S. M. *Semiconductor devices: physics and technology*; John Wiley & Sons: New York, 2008.

(28) Rezaei, M.; Park, M.-S.; Tan, C. L.; Mohseni, H. Sensitivity limit of nanoscale phototransistors. *IEEE Electron Device Lett.* **2017**, *38*, 1051−1054.

(29) Liu, F.; Shimotani, H.; Shang, H.; Kanagasekaran, T.; Zolyomi, V.; Drummond, N.; Fal'ko, V. I.; Tanigaki, K. High-sensitivity photodetectors based on multilayer GaTe flakes. *ACS Nano* **2014**, *8*, 752−760.
(30) Chaves, F. A.; Jiménez, D. Electrostatics of two-dimensional lateral junctions. *Nanotechnology* **2018**, *29*, 275203.
(31) Ilatikhameneh, H.; Ameen, T.; Chen, F.; Sahasrabudhe, H.; Klimeck, G.; Rahman, R. Dramatic impact of dimensionality on the electrostatics of PN junctions and its sensing and switching applications. *IEEE Trans. Nanotechnol.* **2018**, *17*, 293−298.
(32) Liu, L.; Rabinowitz, J.; Bianconi, S.; Park, M.-S.; Mohseni, H. Highly sensitive SWIR detector array based on nanoscale phototransistors integrated on CMOS readout. *Appl. Phys. Lett.* **2020**, *117*, 191102.
(33) Rabinowitz, J.; Rezaei, M.; Park, M.-S.; Tan, C. L.; Ulmer, M.; Mohseni, H. When shot-noise-limited photodetectors disobey Poisson statistics. *Opt. Lett.* **2020**, *45*, 3009−3012.
(34) Memis, O. G.; Katsnelson, A.; Kong, S.-C.; Mohseni, H.; Yan, M.; Zhang, S.; Hossain, T.; Jin, N.; Adesida, I. Sub-Poissonian shot noise of a high internal gain injection photon detector. *Opt. Express* **2008**, *16*, 12701−12706.
(35) Jin, Y.; Wang, J.; Sun, B.; Blakesley, J. C.; Greenham, N. C. Solution-processed ultraviolet photodetectors based on colloidal ZnO nanoparticles. *Nano Lett.* **2008**, *8*, 1649−1653.
(36) Cheng, G.; Wu, X.; Liu, B.; Li, B.; Zhang, X.; Du, Z. ZnO nanowire Schottky barrier ultraviolet photodetector with high sensitivity and fast recovery speed. *Appl. Phys. Lett.* **2011**, *99*, 203105.
(37) Tian, W.; Zhi, C.; Zhai, T.; Chen, S.; Wang, X.; Liao, M.; Golberg, D.; Bando, Y. In-doped $Ga_2O_3$ nanobelt based photodetector with high sensitivity and wide-range photoresponse. *J. Mater. Chem.* **2012**, *22*, 17984−17991.
(38) Wang, X.; Zhang, Y.; Chen, X.; He, M.; Liu, C.; Yin, Y.; Zou, X.; Li, S. Ultrafast, superhigh gain visible-blind UV detector and optical logic gates based on nonpolar a-axial GaN nanowire. *Nanoscale* **2014**, *6*, 12009−12017.
(39) Liu, X.; Gu, L.; Zhang, Q.; Wu, J.; Long, Y.; Fan, Z. All-printable band-edge modulated ZnO nanowire photodetectors with ultra-high detectivity. *Nat. Commun.* **2014**, *5*, 1−9.
(40) Jung, J. H.; Yoon, M. J.; Lim, J. W.; Lee, Y. H.; Lee, K. E.; Kim, D. H.; Oh, J. H. High-Performance UV−Vis−NIR Phototransistors Based on Single-Crystalline Organic Semiconductor−Gold Hybrid Nanomaterials. *Adv. Funct. Mater.* **2017**, *27*, 1604528.
(41) Wu, J. M.; Chang, W. E. Ultrahigh responsivity and external quantum efficiency of an ultraviolet-light photodetector based on a single $VO_2$ microwire. *ACS Appl. Mater. Interfaces* **2014**, *6*, 14286−14292.
(42) Tsai, D.-S.; Liu, K.-K.; Lien, D.-H.; Tsai, M.-L.; Kang, C.-F.; Lin, C.-A.; Li, L.-J.; He, J.-H. Few-layer $MoS_2$ with high broadband photogain and fast optical switching for use in harsh environments. *ACS Nano* **2013**, *7*, 3905−3911.
(43) Jacobs-Gedrim, R. B.; Shanmugam, M.; Jain, N.; Durcan, C. A.; Murphy, M. T.; Murray, T. M.; Matyi, R. J.; Moore, R. L.; Yu, B. Extraordinary photoresponse in two-dimensional $In_2Se_3$ nanosheets. *ACS Nano* **2014**, *8*, 514−521.
(44) Li, Q.; Gao, T.; Wang, Y.; Wang, T. Adsorption and desorption of oxygen probed from ZnO nanowire films by photocurrent measurements. *Appl. Phys. Lett.* **2005**, *86*, 123117.
(45) Gu, Y.; Kwak, E.-S.; Lensch, J.; Allen, J.; Odom, T. W.; Lauhon, L. J. Near-field scanning photocurrent microscopy of a nanowire photodetector. *Appl. Phys. Lett.* **2005**, *87*, 043111.
(46) Bonakdar, A.; Mohseni, H. Impact of optical antennas on active optoelectronic devices. *Nanoscale* **2014**, *6*, 10961−10974.
(47) Bonakdar, A.; Mohseni, H. Hybrid optical antenna with high directivity gain. *Opt. Lett.* **2013**, *38*, 2726−2728.
(48) Wu, W.; Bonakdar, A.; Mohseni, H. Plasmonic enhanced quantum well infrared photodetector with high detectivity. *Appl. Phys. Lett.* **2010**, *96*, 161107.


https://doi.org/10.1021/acs.nanolett.1c03665
*Nano Lett.* XXXX, XXX, XXX−XXX